

Effect of neutral donor scattering on the time-dependent exciton-polariton photoluminescence line shape in GaAs

T. Steiner* and M. L. W. Thewalt

Department of Physics, Simon Fraser University, Burnaby British Columbia, Canada V5A 1S6

E. S. Koteles and J. P. Salerno

GTE Laboratories, Inc., Waltham, Massachusetts 02254

(Received 10 February 1986)

The importance of neutral donor scattering on the observed time-resolved exciton-polariton line shape in GaAs at low temperatures is demonstrated. Samples which in continuous excitation luminescence show a single polariton peak can have substantially different line shapes at short delay times after excitation with mode-locked laser pulses. A series of time-resolved spectra show at short delays after the laser pulses a doublet line shape which gradually transforms into a singlet with longer delays. We have explained this phenomenon as arising from the delay in arrival at the sample surface of polaritons in the energy region corresponding to the central "dip" due to neutral donor scattering. A time-dependent Boltzmann-equation model of polariton transport in the crystal incorporating only elastic neutral donor scattering has been constructed to simulate the experimental results.

INTRODUCTION

In direct-band-gap semiconductors with dipole-active excitons there exists a strong coupling of free excitons with photons of the same energy. This coupling, as pointed out by Hopfield,¹ results in a mixed-mode excitation called an exciton-polariton. The coupling opens up a gap at the crossing point of the exciton and photon dispersion curves resulting in a two branch polariton dispersion curve given by

$$\left(\frac{\hbar ck}{E}\right)^2 = \epsilon_0 + \frac{2\epsilon_0 E_{LT} E}{E_0^2(k) - E^2}, \quad (1)$$

where ϵ_0 is the dielectric constant in the absence of polaritons, E_{LT} , the splitting between the uncoupled longitudinal and transverse excitons at $k=0$, is a measure of the coupling strength, E is the polariton energy, and $E_0(k)$ is the energy of the uncoupled free exciton of wave vector k given by the transverse exciton energy E_T plus the kinetic energy. In the near resonance region, [$E_0(k) - E \ll E$], the dispersion relation can be approximated by

$$\left(\frac{\hbar ck}{E}\right)^2 = \epsilon_0 + \frac{\epsilon_0 E_{LT}}{E_0(k) - E}. \quad (2)$$

The polariton dispersion curve appropriate for GaAs is presented in Fig. 1(a). On the lower branch (LPB), at large wave vectors, the polaritons are predominantly excitonlike, whereas at small wave vectors they are photonlike. On the upper branch (UPB) the polaritons start out excitonlike but rapidly become photonlike with increasing wave vector.

The nature of the polariton dispersion relation has a profound effect on the luminescence mechanism in this energy region.^{1,2} Note that the lower polariton branch

does not have a minimum energy. Excitonlike polaritons can be inelastically scattered to the lower energy photonlike region of the dispersion curve. These photonlike polaritons interact only weakly with the lattice and thus rapidly exit the crystal. Toyozawa² predicted that in the knee region of the dispersion curve a "bottleneck" to further inelastic scattering to lower energy would result due to a lack of suitable small wave vector photons and the small density of final states in the photonlike region of the dispersion curve. The existence of this bottleneck has been experimentally verified with time-resolved photoluminescence.^{3,4} Due to this bottleneck, a quasithermal equilibrium distribution of polaritons can then be established above the knee of the dispersion curve. The group velocity of polaritons on the lower branch, $v(E) = \hbar^{-1} dE/dk$, varies very rapidly with energy,⁵ and has a minimum just above the knee [Fig. 1(b)]. Velocity-dependent scattering processes are greatly enhanced in this energy region. This enhancement in scattering together with the low group velocity results in much slower diffusion of these polaritons.

For uncoupled free excitons, no-phonon luminescence can only result if an almost stationary exciton of the same wave vector as light of that energy annihilates, giving up its energy to a photon which then travels unhindered to the surface to emerge as luminescence. In the case of polaritons the distinction between the exciton and photon cannot be made since excitations in this energy region are inherently mixed. No-phonon polariton luminescence results from those polaritons which upon reaching the surface, are converted into photons external to the crystal. Thus, a theoretical description of polariton luminescence becomes a transport problem.⁶ This introduces considerable complexity to the luminescence problem, with the net result that the experimentally observed no-phonon polari-

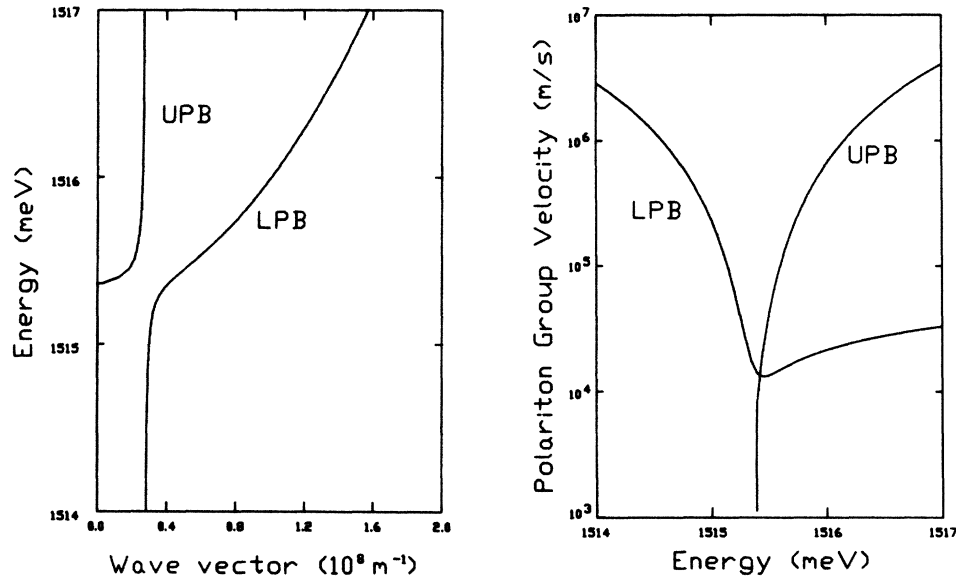


FIG. 1. (a) The polariton dispersion curves for GaAs calculated using the parameters given in the text and Eq. (2). The upper (UPB) and lower (LPB) polariton branches are labeled. (b) The LPB and UPB group velocities calculated from Eq. (2).

ton luminescence line shape does not necessarily reflect the population distribution of polaritons inside the crystal.

The usual, experimentally observed exciton-polariton spectrum is a doublet, rather than the singlet expected from the quasiequilibrated polariton population above the knee in the lower branch of the dispersion curve.⁷ This doublet structure has been interpreted in many ways. Gross *et al.*⁸ explained the higher energy polariton peak in CdS as arising from a minimum in the reflectivity of the surface at this energy. Sell *et al.*⁹ attributed the doublet polariton spectrum in GaAs to emission from the two polariton branches. Alternatively, the doublet has been attributed to the scattering of polaritons by free electrons,¹⁰ or to intrinsic reabsorption (meaning scattering from phonons^{2,11}) of polaritons moving towards the surface.¹²⁻¹⁴ It has also been suggested that polariton impurity scattering is the dominant scattering mechanism at low temperatures.¹⁵ Recently it has been experimentally shown that elastic neutral donor scattering has a marked effect on the polariton luminescence line shape, and is consequently the scattering mechanism responsible for the "reabsorption," where "absorption" is broadly defined as requiring only a change in direction of the polaritons.¹⁶⁻¹⁸ Very recently it has been suggested that the dip in the polariton spectrum is due to absorption caused by a surface electric field modified polariton resonance.¹⁹ We shall present some experimental evidence which makes this last explanation unlikely for our samples. We will suggest an alternative explanation of their experimental results. However, it is important to understand the complexity of the problem and hence the limitations of a simplified model. Any mechanism which affects the transport of polaritons to the sample surface, the probability of transmission at the surface, the distribution of polaritons in the crystal, or the polariton energy distribution can in-

fluence the observed polariton luminescence. Consequently, one can expect great variations in the observed emission with different samples, surface preparation, or experimental conditions.

In this paper we will present evidence attesting to the importance of neutral donor scattering to the time-resolved polariton spectrum of a variety of GaAs samples grown by molecular beam epitaxy (MBE) whose cw photoluminescence spectra have already been reported.¹⁶⁻¹⁸ In the first section of this paper we will present the experimental results, followed by a time-dependent Boltzmann-equation model of the polariton transport, and finally a discussion of these and other results.

EXPERIMENTAL PROCEDURE

The photoluminescence was excited using a mode-locked, Ar-ion laser, synchronously pumping a dye laser. This resulted in < 10 ps pulses, at either 590 nm, well above the gap of GaAs, or around 820 nm for resonant excitation. The intrinsic repetition rate of 80 MHz set by the ion laser cavity length was reduced to 4 MHz using a cavity dumper. The laser pulse train was directed onto the front surface of a MBE GaAs crystal immersed in superfluid He. The resultant luminescence was analyzed using a double $\frac{3}{4}$ m spectrometer and subsequently detected by a fast photomultiplier (Varian VPM159A3) operated in the photon counting mode. The luminescence photon-generated pulse provides the start signal to a time-to-amplitude converter. The stop pulse is provided by an avalanche photodiode sampling part of the incident beam. The output of the time-to-amplitude converter is analyzed by a microcomputer based pulse-height analyzer, which redirects the photon counts into up to eight separate bins depending on the time difference between the start and

stop pulses. This allows the simultaneous collection of eight spectra corresponding to adjacent, variable time windows during and after the laser pulse. The time resolution of this system is limited by the response time of the photomultiplier, which in conjunction with our timing electronics, has a FWHM of < 250 ps in response to a train of mode-locked laser pulses.

Using cw photoluminescence Koteles *et al.*¹⁶ have shown that the shape of the polariton luminescence depends strongly on the neutral donor concentration. A series of samples, with progressively smaller donor concentrations, as determined by the relative strengths of polariton and donor bound exciton luminescence, showed a change from the usual doublet polariton line shape to a narrow single line. In this paper we present the results of time-resolved measurements on these same samples. In order of decreasing donor concentration these are MBE 3-7, MBE 3-14, and MBE 3-9. Figure 2(b) depicts a series of time-resolved spectra using above band-gap excitation of sample MBE 3-14 which, under cw excitation, exhibits only a single polariton peak. Here we see the evolution of the polariton line shape from a doublet at short delay times after the laser pulses, to a singlet at longer delays. Other samples, with even lower donor concentrations, such as MBE 3-9 have only a single peak at all times [Fig. 2(c)], whereas others with higher donor concentrations (e.g., MBE 3-3), always have a doublet regardless of the time delay [Fig. 2(a)].

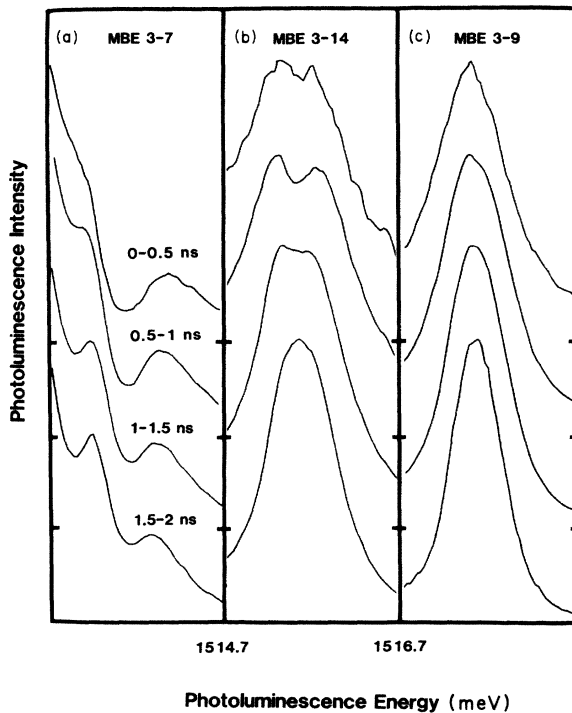


FIG. 2. A series of time-resolved spectra using 0.5 ns windows of three different samples with decreasing neutral donor concentration going from (a) to (c). Sample temperature was ~ 1.8 K and the average excitation density was 500 mW/cm² corresponding to a peak power of ~ 10 kW/cm². (b) shows the time evolution of the dip in a sample with moderate neutral donor concentration.

The qualitative features of the time-resolved polariton line shape were not found to depend on the excitation density for either the low donor concentration samples, which never showed a dip, or the high donor concentration samples, which always had a doublet polariton peak. For the intermediate donor concentrations, there was, however, a considerable dependence on the excitation density, as shown in Fig. 3(b). For these samples it was found that low excitation densities produced narrow, singlet polariton line shapes, while higher excitation produced the broader, doublet structure. Resonant excitation at the $n = 2$ polariton excited state energy was also found to produce results considerably different from those previously described for nonresonant above-band-gap excitation. With resonant excitation of the polaritons, *all* the samples showed a singlet polariton peak. An example of this excitation energy dependence is shown in Fig. 3(a). We shall propose tentative explanations of these observations in the next section.

A careful examination of the transient characteristics of the luminescence as a function of photon energy in those samples showing a doublet polariton structure provides strong evidence supporting the neutral donor scattering delay model. In Fig. 4 the luminescence intensities versus delay time for three different luminescence energies are shown for above-band-gap excitation of sample MBE 3-14. The three luminescence energies correspond to the two peaks of the polariton doublet, 1515.3 and 1515.7 meV, and to

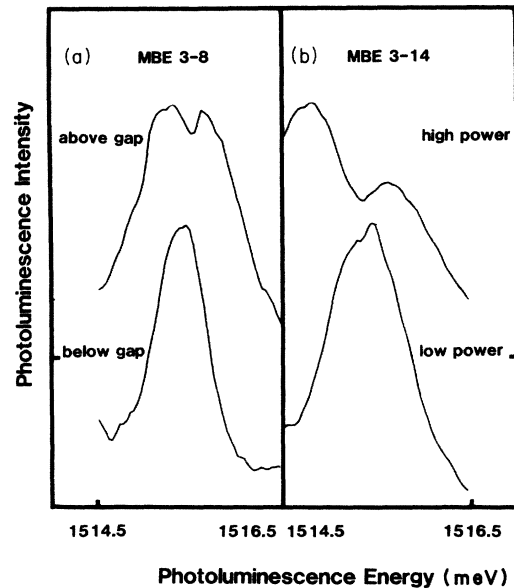


FIG. 3. (a) A comparison of the exciton-polariton spectra resulting from excitation by above- and below-band-gap radiation. The top spectrum was collected while pumping above the gap with an excitation density of ~ 500 mW/cm² with the sample immersed in superfluid He. The bottom spectrum was collected under identical experimental conditions except that the first excited state of the polariton was resonantly pumped. (b) demonstrates the effect of above band-gap excitation density on the polariton spectrum. The top and bottom spectra were collected using average excitation densities of 2 W/cm² and 200 mW/cm² respectively. All spectra were taken in the time window 0.5 – 1 ns after excitation.

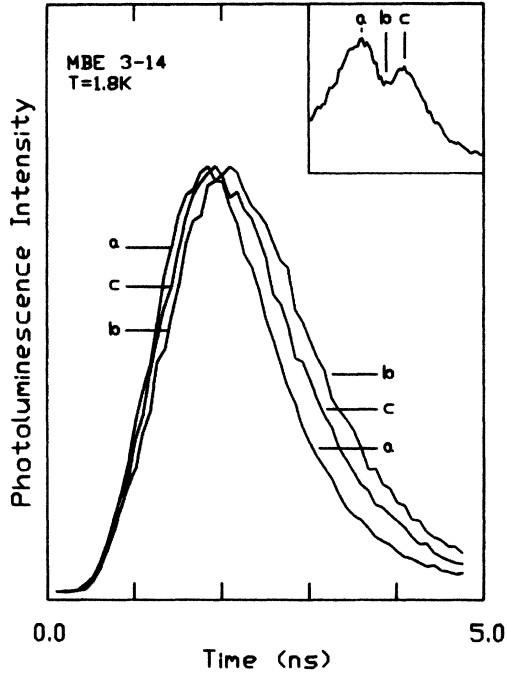


FIG. 4. These traces are the measured, time-dependent photoluminescence curves in the polariton energy region. The top right inset shows the 0.5–1.0 ns spectrum of MBE 3–14 as in Fig. 2 indicating at which energy the three measurements were done. (a) below the dip in energy, (b) at the dip energy, and (c) above the dip in energy.

the dip region in between these peaks at 1515.5 meV. As can be seen in Fig. 4, the most noticeable difference between the transient behavior of polaritons in the dip region as compared to the two peak regions is that the luminescence in the dip region builds up more slowly. This is exactly what would be expected from our model, since it is precisely these polaritons in the dip energy which are delayed in reaching the sample surface due to the enhanced neutral donor scattering cross section and reduced group velocity.

THEORY

The impurity elastic scattering cross section for polaritons can be determined from the bare free exciton cross section as pointed out by Hopfield.²⁰ Using Fermi's golden rule the differential bare exciton scattering cross section can be written as²⁰

$$\frac{d\sigma}{d\Omega} = \frac{2\pi}{\hbar v_{\text{ex}}} |\langle k' | V | k \rangle|^2 \rho(k'), \quad (3)$$

where v_{ex} is the mechanical exciton velocity. For elastic, s -wave scattering, the matrix element depends only on the energy of the exciton. The total scattering cross section can thus be written as

$$\begin{aligned} \sigma_{\text{ex}}(E) &= \frac{8\pi^2}{\hbar v_{\text{ex}}} |\langle E | V | E \rangle|^2 \rho_{\text{ex}}(E) \\ &= 4 |\langle E | V | E \rangle|^2_{\text{ex}} \frac{k_{\text{ex}}^2}{\hbar^2 v_{\text{ex}}^2}. \end{aligned} \quad (4)$$

For polariton scattering there are, in general, two bands for a given energy and thus elastic, interband scattering is possible. The polariton elastic scattering cross section can be written as^{20,21}

$$\begin{aligned} \sigma_{\pi}(E) &= \frac{8\pi^2}{\hbar v_i} |\langle E | V | E \rangle|^2 \rho_r(E) \\ &= 4 |\langle E | V | E \rangle|^2_P \frac{k_r^2}{\hbar^2 v_i v_r}. \end{aligned} \quad (5)$$

Here i and r are the initial- and final-state band indices. The matrix element, velocity, and density of states now correspond to polariton, rather than bare exciton quantities. The polariton-group velocity and final density of states

$$\rho(E) = \frac{1}{2\pi^2} \frac{k^2(E)}{\hbar v(E)} \quad (6)$$

can be calculated from the dispersion relation [Eq. (2)]. The polariton scattering matrix element is related to the bare exciton matrix element by

$$|\langle E | V | E \rangle|^2_P = |\langle E_k | V | E_k \rangle|^2_{\text{ex}} |\phi(r, i)|^2, \quad (7)$$

where $\phi(r, i)$ corresponds to the overlap of the exciton portion of the initial- and final-state polariton wave functions. This can be evaluated using Hopfield's c parameters^{22,4} and was found to be essentially equal to 1 in the whole region of interest, for both interband and intraband scattering. The polariton wave function is thus almost completely excitonlike, but its group velocity is not.²⁰ E_k is the kinetic energy of the initial polariton given by $E_k = 1/2 m_{\text{ex}} v_i^2$. Equation (5) can thus be rewritten as

$$\sigma_{\pi}(E) = \sigma_{\text{ex}}(E_k) \left(\frac{k_r(E)}{k_{\text{ex}}} \right) \frac{v_{\text{ex}}^2(E)}{v_r(E) v_i(E)}, \quad (8)$$

where k_{ex} and v_{ex} are the bare exciton wave vector and velocity, respectively. The matrix element is evaluated for the kinetic energy of the incident polariton. Hence $v_{\text{ex}} = v_i$ and Eq. (8) becomes

$$\sigma_{\pi}(E) = \sigma_{\text{ex}}\left(\frac{1}{2} m_{\text{ex}} v_i^2\right) \left(\frac{k_r(E)}{k_{\text{ex}}} \right) \frac{v_i(E)}{v_r(E)}. \quad (9)$$

Again $k_b(E)$ and $v_b(E)$ are calculated for a given polariton energy and branch using Eq. (2). Lee *et al.*¹⁸ have calculated the exciton elastic scattering cross section using partial wave analysis. These results indicated that s -wave scattering is predominant and that neutral donor scattering is at least an order of magnitude larger than neutral acceptor scattering at all energies. This result is reasonable on physical grounds. Since the donor binding energy in GaAs is much smaller than the acceptor binding energy, the neutral donor wave function is much more extended in space, and hence should provide a larger scattering cross section. The neutral donor scattering cross section for polaritons has a peak in the bottleneck region, which, coupled with the smaller group velocity in this energy region, results in a delay in the arrival of these polaritons at the surface. In cw luminescence, this creates a dip in the exciton-polariton spectrum of samples with large donor

concentrations, since on their slower journey to the sample surface inelastic scattering or trapping mechanisms have more time to depopulate polaritons in this energy region. In time-resolved photoluminescence, however, this mechanism can lead to a time-dependent dip in more lightly doped samples. At short times more of the faster traveling, less scattered polaritons above and below the dip energy region reach the surface. At longer times the more populous dip energy-region polaritons reach the surface, giving rise to a spectrum more indicative of the population distribution. In these more lightly doped samples, even the dip energy polaritons reach the surface before being inelastically scattered out of this energy region. Unlike the cw luminescence case, the existence of the dip at short delay times in these samples does not depend on inelastic scattering mechanisms, but on the arrival delay of the dip region polaritons. For very small neutral donor concentrations all the polaritons diffuse rapidly and no dip is observed, even at short time delays. The observation that the magnitude of the dip decreases with decreasing above-band-gap excitation density can be qualitatively explained, since the penetration depth of the polaritons would decrease, resulting in an initial spatial distribution with its centroid closer to the sample surface. Similarly, below-gap excitation, resonantly creating $n=2$ polaritons, also results in an initial polariton distribution closer to the surface. Such a distribution results in a much reduced arrival delay at the surface for polaritons of all energies. This results in a single peak polariton spectrum at all delay times, even for samples having substantial donor concentrations, since there is insufficient time for inelastic scattering processes to significantly reduce the population in the dip energy region. The effect of the initial distribution on the observed exciton-polariton line shape has also been studied using cw excitation.¹⁸

We have constructed a model of polariton luminescence using a time-dependent Boltzmann equation and considering only elastic neutral donor scattering. This model intrinsically allows for multiple scattering events in contrast to previous treatments of polariton luminescence with neutral donor scattering under cw excitation.¹⁶⁻¹⁸ The observed photon intensity, $I(E,t)$ is given by the equation

$$I(E,T)d\Omega(E)dE = \sum_{b=1}^2 T_b(E,\Omega)[\mathbf{v}_b(E,\Omega) \cdot \Omega] \times N_b(x=0, \mathbf{v}_b(E), t) \frac{d\Omega(E)}{n_b^2} dE. \quad (10)$$

Here b is the branch index, n_b the refractive index calculated from Eq. (2), $T_b(E,\Omega)$ is the transmissivity of the surface, $v_b(E)$ is the polariton-group velocity, $N_b(x=0, v_b(E), t)$ is the polariton number density distribution function at the sample surface, and Ω is the angular direction of detection.

The existence of the two polariton branches complicates the calculation of the transmission function since the Fresnel equations no longer provide sufficient boundary conditions. Additional boundary conditions (ABC) must be supplied.²² Following Askary and Yu^{4,7} we have cal-

culated the transmission and reflection coefficients using the Pekar ABC (Ref. 23). The transmission function of the LPB decreases rapidly above E_L whereas the transmission of the UPB increases. Luminescence from the energy region above E_L is thus primarily from the UPB. The polaritons of the upper branch, due to their large velocity and small scattering cross section, provide a path whereby LPB polaritons can rapidly escape the crystal if a mechanism for populating the UPB states exists. This scattering mechanism is provided by elastic neutral donor scattering. In crystals having large concentrations of neutral donors, polaritons having energies either above or below the dip energy region have a means of rapidly reaching the sample surface. Polaritons in the dip energy region are, however, impeded from diffusing to the surface by neutral donor scattering. This results in a doublet line shape. In samples with lower neutral donor concentrations, dip polaritons reach the surface more easily, while higher energy LPB polaritons cannot easily be scattered to the UPB, hindering their escape from the crystal resulting in a single polariton peak.

As has been pointed out by Travnikov and Krivolapchuk⁶ for the cw time-independent case, the solution of Eq. (10) hinges on calculating the distribution function N at the sample surface. In other words, the luminescence problem becomes a polariton transport problem. Considering only one branch for the moment, the time-dependent Boltzmann equation for the distribution function N can be written as

$$\frac{dN(x, \mathbf{v}, t)}{dt} = \int [N(x, \mathbf{v}', t) - N(x, \mathbf{v}, t)] Q(\mathbf{v}', \mathbf{v}) d^3 v' - \mathbf{v} \cdot \nabla_x N(x, \mathbf{v}, t). \quad (11)$$

Here $Q(\mathbf{v}', \mathbf{v})$ is the scattering rate of polaritons from velocity \mathbf{v} to velocity \mathbf{v}' . Since we shall consider only isotropic, elastic, pure s -wave scattering, Q is independent of the directions $Q(\mathbf{v}', \mathbf{v}) = \Gamma(E)$. We shall consider a semi-infinite crystal, and hence only motion perpendicular to the sample surface is important. This allows Eq. (11) to be transformed into a quasi-one-dimensional equation:

$$\frac{dN(x, E, \theta, t)}{dt} = \Gamma(E) \int_0^\pi [N(x, E, \theta', t) q(\theta, \theta') - N(x, E, \theta, t) q(\theta', \theta)] d\theta - v \cos\theta \frac{dN(x, E, \theta, t)}{dx}, \quad (12)$$

where θ is the angle between the direction of polariton propagation and the positive x axis which points into the crystal. Γ is the scattering rate, while q is the angular dependence of the transition rate introduced by the geometrical factors resulting from the change in variables. Since only elastic scattering is being considered, polaritons of different energies are not coupled by Eq. (12) and hence Eq. (12) can be separately calculated for each energy value. The explicit energy dependence will be dropped from the equation. For s -wave scattering $q(\theta, \theta')$ can be simply evaluated by considering the fraction of the total 4π solid angle represented by the final polariton direction θ . Hence q becomes

$$q(\theta, \theta') d\theta = \frac{2\pi \sin\theta}{4\pi} d\theta = \frac{1}{2} \sin\theta d\theta. \quad (13)$$

q is no longer symmetric in this space and only depends on the final angle. Equation (12) can thus be rewritten in the form

$$\frac{dN(x, \theta, t)}{dt} = \frac{1}{2} \Gamma \sin(\theta) G(x, t) - (\Gamma + 1/\tau) N(x, \theta, t) - v \cos(\theta) \frac{dN(x, \theta, t)}{dx}, \quad (14)$$

$$\begin{aligned} \frac{dN_1(x, \theta, t)}{dt} &= \frac{1}{2} \sin\theta [\Gamma_{12} G_2(x, t) + \Gamma_{11} G_1(x, t)] - (\Gamma_{11} + \Gamma_{21} + 1/\tau) N_1(x, \theta, t) - v_1 \cos\theta \frac{dN_1(x, \theta, t)}{dx}, \\ \frac{dN_2(x, \theta, t)}{dt} &= \frac{1}{2} \sin\theta [\Gamma_{21} G_1(x, t) + \Gamma_{22} G_2(x, t)] - (\Gamma_{22} + \Gamma_{12} + 1/\tau) N_2(x, \theta, t) - v_2 \cos\theta \frac{dN_2(x, \theta, t)}{dx}, \end{aligned} \quad (16)$$

where Γ_{ri} is the transition rate from initial branch i to final branch r . We have solved this set of equations numerically, for a number of energies in the polariton region of the spectrum, with different neutral donor concentrations.

To solve this equation, one needs to assume a reasonable initial distribution function N_0 . This initial distribution is completely unknown but the qualitative results are not greatly dependent on the functional form chosen for the distribution. The spatial distribution should be peaked in the bulk of the sample with all directions of propagation equally probable, while the energy distribution should be peaked in the dip region. For simplicity, N_0 has been assumed to be separable into an energy distribution and a spatial distribution⁶ given by

$$n(x) = \frac{1}{L_0 - L_1} [\exp(-x/L_0) - \exp(-x/L_1)]. \quad (17)$$

Here L_0 is the characteristic generation length of free carriers by the incident light and L_1 is the surface recombination length of free carriers due to free carrier traps at the sample surface which deplete the carrier concentration near the surface and hence also the polariton density. For the energy distribution we assumed a Gaussian peaked at E_p of width E_w . The procedure for evaluating Eq. (16) is as follows. For a given energy, calculate the group velocities using Eq. (2). then using these velocities calculate the transition rates Γ_{ri} using

$$\Gamma_{ri}(E) = N_D \sigma_{ri}(E) v_i(E), \quad (18)$$

where N_D is the concentration of neutral donors and σ is the scattering cross section of Eq. (9). In this step we have used the exciton cross sections calculated by Lee *et al.*¹⁸ Equations (16) are then converted into finite-difference form, and the time evolution calculated numerically. A series of time-resolved spectra, for comparison with experiment, are then generated by convoluting these calculated luminescence curves with a realistic instrument response and summing the luminescence for the duration of the desired time windows. The results for three different neutral donor concentrations are depicted in Fig. 5. The parameters used to generate these spectra are

where $G(x, t)$ is given by

$$G(x, t) = \int_0^\pi N(x, \theta', t) d\theta'. \quad (15)$$

An energy-independent trapping term, corresponding to a pure exponential decay with a phenomenological trapping time τ , has been added to the loss term in Eq. (14). However, being energy independent, it cannot change the shape of the observed polariton distribution. Reintroducing the second polariton branch, and allowing for interbranch scattering changes Eq. (14) into two coupled equations for energies above E_L

$$\begin{aligned} m_{ex} &= 0.55 m_0, \\ \epsilon_0 &= 12.8, \\ E_{LT} &= 0.07 \text{ meV}, \\ E_T &= 1515.3 \text{ meV}, \\ E_P &= 1515.35 \text{ meV}, \\ E_W &= 0.5 \text{ meV}, \\ L_0 &= 1.0 \mu\text{m}, \\ L_1 &= 0.25 \mu\text{m}. \end{aligned}$$

DISCUSSION

L_0 was set to the approximate above-band-gap absorption length of GaAs while L_1 was arbitrarily set to 0.25 μm , a value which produced results resembling the experimental observations in Fig. 2. It is clear that the polariton spectrum depends drastically on the initial population distribution of polaritons. If the surface recombination length L_1 were reduced there would be a decreased time-dependent dip, since there would be a greater number of polaritons of all energies near the surface, leading to instantaneous luminescence at all polariton energies. The polariton spatial distribution would also have a large effect in cw photoluminescence, since a short surface recombination length would reduce the time available for the inelastic scattering mechanisms to reduce the number of dip energy-region polaritons reaching the surface. We feel that the effects of surface preparation^{19,24} on the luminescence spectrum enter in this way. Cleavage of a GaAs sample in ultra high vacuum²⁴ causes a disappearance of the dip during luminescence measurements, although subsequent exposure to air reestablishes the dip. This effect can easily be explained, as was done by the authors, by invoking surface states. Since the number of surface traps after cleavage in UHV is far lower than for a contaminated surface, L_1 will be decreased. The important effect of the spatial distribution of polaritons was also realized by Weisbuch and Ulbrich¹³ in the interpreta-

tion of their experimental results. The effect of surface electric field on the polariton line shape¹⁹ can also be interpreted along these lines.

The observed dip increases with increasing electric field.¹⁹ The surface field separates the photo-generated holes and electrons hindering polariton formation in the surface region. This would serve to increase L_1 by a different mechanism, but with the same final result of increasing the distance to the surface for all polaritons, and hence increased scattering for those in the bottleneck energy region. Schultheis and Tu¹⁹ have, however, argued that their results should be interpreted as arising due to an electric field modified polariton resonance near the surface. Our experimental results show that this mechanism is not applicable in our samples. Figure 3(b) shows the disappearance of the dip with decreased excitation power. Their proposed mechanism would predict the opposite, since an increase in excitation density would generate more free carriers which would discharge the deep surface traps responsible for the surface electric field, resulting in a reduced dip.

The results of the Boltzmann-equation model do not exactly reproduce the experimental spectra. The main reason for the discrepancy is the omission of inelastic scattering processes in the model. This is not a rigorously justifiable simplification since inelastic scattering processes tend to repopulate those polaritons below the bottleneck, and in the UPB, which rapidly exit the crystal. The omission of these processes results in the calculated peaks being too narrow at long times, particularly for the low donor concentration case. Furthermore, with only elastic scattering, the single peak polariton spectrum is established after long enough delays regardless of the neutral donor concentration, since elastic scattering can only delay the arrival time of the polaritons at the surface, but cannot redistribute the population. A complete theory would also require a more realistic initial energy distribution, calculated using inelastic scattering rates. Nevertheless, these results clearly illustrate the important effect of elastic neutral donor scattering on the exciton-polariton photoluminescence line shape of GaAs. We would like to reiterate however, that polariton luminescence is a compli-

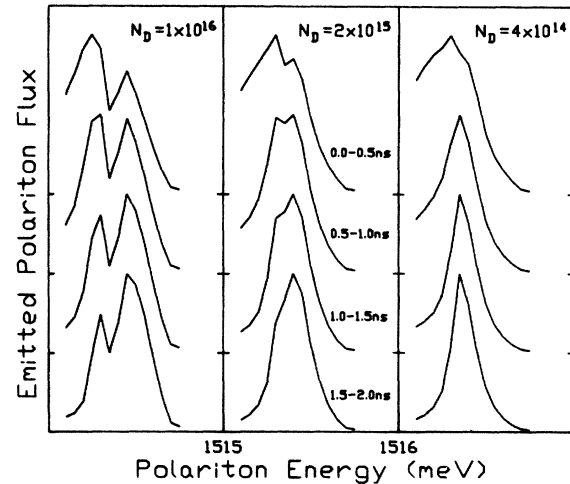


FIG. 5. A series of time-resolved spectra generated by the Boltzmann-equation model using identical parameters except for the neutral donor concentration. (a) $N_D = 10^{16}/\text{cm}^3$, (b) $N_D = 2 \times 10^{15}/\text{cm}^3$, and (c) $N_D = 4 \times 10^{14}/\text{cm}^3$.

cated transport problem with nontrivial boundary conditions. Consequently, any mechanism that affects the initial distribution either in space or in energy, the transport of the polaritons in the crystal, or the nature of the crystal boundary itself, can modify the experimentally observed polariton spectrum. Thus no single mechanism can explain the huge variety of observed polariton spectra in different crystals. It is clear, however, that a comprehensive theory of polariton luminescence must include the effect of elastic scattering from neutral impurities.

ACKNOWLEDGMENTS

This work has been carried out with financial support of the Natural Sciences and Engineering Research Council of Canada. T.S. thanks the council for financial support. M.L.W.T. gratefully acknowledges the support by the Alfred P. Sloan Foundation.

*Present address: IBM Thomas J. Watson Research Center, P.O. Box 218, Yorktown Heights, NY 10598.

¹J. J. Hopfield, Phys. Rev. **112**, 1555 (1958).

²Y. Toyozawa, Prog. Theor. Phys. Suppl. **12**, 111 (1959).

³U. Heim and P. Wiesner, Phys. Rev. Lett. **30**, 1205 (1973); P. Wiesner and U. Heim, Phys. Rev. B **11**, 3071 (1975).

⁴F. Askary and P. Y. Yu, Phys. Rev. B **31**, 6643 (1985).

⁵R. G. Ulbrich and G. W. Fehrenbach, Phys. Rev. Lett. **43**, 963 (1979).

⁶V. V. Travnikov and V. V. Krivolapchuk, Zh. Eksp. Teor. Fiz. **85**, 2087 (1983) [Sov. Phys.—JETP **58**, 1210 (1983)].

⁷F. Askary and P. Y. Yu, Solid State Commun. **47**, 241 (1983).

⁸E. Gross, S. Permogorov, V. Travnikov, and A. Selkin, Solid State Commun. **10**, 1071 (1972).

⁹D. D. Sell, S. E. Stokowski, R. Dingle, and J. V. DiLorenzo, Phys. Rev. B **7**, 4568 (1973).

¹⁰K. Aoki, Phys. Lett. **72A**, 63 (1979).

¹¹W. C. Tait and R. L. Weiher, Phys. Rev. **178**, 1404 (1969).

¹²C. Weisbuch and R. G. Ulbrich, Phys. Rev. Lett. **39**, 654 (1977).

¹³C. Weisbuch and R. G. Ulbrich, J. Lumin. **18/19**, 27 (1979).

¹⁴V. V. Travnikov and V. V. Krivolapchuk, Pis'ma Zh. Eksp. Teor. Fiz. **37**, 355 (1983) [Sov. Phys.—JETP Lett. **37**, 419 (1983)].

¹⁵C. Weisbuch and R. G. Ulbrich, J. Lumin. in *Festkörperprobleme* (Advances in Solid State Physics), edited by J. Treusch (Vieweg, Braunschweig, 1978), Vol. XVIII, p. 217.

¹⁶E. S. Koteles, J. P. Salerno, W. Bloss, and E. M. Brody, in *Proceedings of the 17th International Conference on the Physics of Semiconductors*, edited by J. D. Chadi and W. A. Harrison (Springer-Verlag, New York, 1985), p. 1247.

¹⁷E. S. Koteles, J. Lee, J. P. Salerno, and M. O. Vassell, Phys. Rev. Lett. **55**, 867 (1985); J. Lee, E. S. Koteles, M. O. Vassell,

- and J. P. Salerno, *J. Lumin.* **34**, 63 (1985).
- ¹⁸W. Bloss, E. S. Koteles, E. M. Brody, B. J. Sowell, J. P. Salerno, and J. V. Gormley, *Solid State Commun.* **54**, 103 (1985).
- ¹⁹L. Schultheis and C. W. Tu, *Phys. Rev. B* **32**, 6978 (1985).
- ²⁰J. J. Hopfield, *Phys. Rev.* **182**, 945 (1969).
- ²¹H. Sumi, *J. Phys. Soc. Jpn.* **41**, 526 (1976).
- ²²For a review, see J. L. Birman and E. L. Ivchenko, in *Excitons*, edited by E. I. Rashba and M. D. Sturge (North-Holland, Amsterdam, 1982), Chaps. 2 and 4, respectively.
- ²³S. I. Pekar, *Zh. Eksp. Teor. Fiz.* **33**, 1022 (1958); **34**, 1176 (1958) [*Sov. Phys.—JETP* **6**, 785 (1958); **7**, 813 (1958)].
- ²⁴B. Fisher and H. J. Stolz, *Appl. Phys. Lett.* **40**, 56 (1982).